Human cystatin C, an amyloidogenic protein, dimerizes through three-dimensional domain swapping

Janowski, Robert; Kozak, Maciej; Jankowska, Elzbieta; Grzonka, Zbigniew; Grubb, Anders; Abrahamson, Magnus; Jaskolski, Mariusz

Published in:
Nature Structural Biology

DOI:
10.1038/86188

2001

1. Jurica, M.S. & Stoddard, B.L. *Cell. Mol. Life Sci.* **55**, 1304–1326 (1999).
2. Belfort, M. & Roberts, R.J. *Nucleic Acids Res.* **25**, 3379–3388 (1997).
3. Belfort, M. & Perlman, P.S. *J Biol. Chem.* **270**, 30237–30240 (1995).
4. Lambowitz, A.M. & Belfort, M. *Annu. Rev. Biochem.* **62**, 587–622 (1993).
5. Dalgaard, J.Z. *et al. Nucleic Acids Res.* **25**, 4626–4638 (1997).
6. Durrenberger, F., Thompson, A.J., Herrin, D.L. & Rochaix, J.D. *Nucleic Acids Res.* **24**, 3323–3331 (1996).
7. Turmel, M., Otis, C., Cote, V. & Lemieux, C. *Nucleic Acids Res.* **25**, 2610–2619 (1997).
8. Argast, G.M., Stephens, K.M., Emond, M.J. & Monnat, R.J., Jr. *J Mol. Biol.* **280**, 345–353 (1998).
9. Marshall, P. & Lemieux, C. *Nucleic Acids Res.* **20**, 6401–6407 (1992).
10. Heath, P.J., Stephens, K.M., Monnat, R.J., Jr. & Stoddard, B.L *Nature Struct. Biol.* **4**, 468–476 (1997).
11. Silva, G.H., Dalgaard, J.Z., Belfort, M. & Van Roey, P. *J. Mol. Biol.* **286**, 1123–1136 (1999).
12. Ichiyanagi, K., Ishino, Y., Ariyoshi, M., Komori, K. & Morikawa, K. *J. Mol. Biol.* **300**, 889–901 (2000).
13. Duan, X., Gimble, F.S. & Quiocho, F.A *Cell* **89**, 555–564 (1997).
14. Komori, K., Ichiyanagi, K., Morikawa, K. & Ishino, Y. *Nucleic Acids Res.* **27**, 4175–4182 (1999).
15. Hu, D., Crist, M., Duan, X. & Gimble, F.S. *Biochemistry* **38**, 12621–12628 (1999).
16. Pingoud, V. *et alJ. Biol. Chem*. **274**, 10235–10243 (1999).
17. Aagaard, C., Awayez, M.J. & Garrett, R.A. *Nucleic Acids Res.* **25**, 1523–1530 (1997).
18. Wende, W., Grindl, W., Christ, F., Pingoud, A. & Pingoud, V. *Nucleic Acids Res.* **24**, 4123–4132 (1996).
19. Lykke-Andersen, J., Garrett, R.A. & Kjems, J. *Nucleic Acids Res.* **24**, 3982–3989 (1996).
20. Jurica, M.S., Monnat, R.J., Jr. & Stoddard, B.L. *Mol. Cell* **2**, 469–476 (1998).
21. Gimble, F. S. & Stephens, B. W. *J. Biol. Chem*. **270**, 5849–5856 (1995).
22. Seligman, L.M., Stephens, K.M., Savage, J.H. & Monnat, R.J., Jr. *Genetics* **147**, 1653–1664 (1997).
23. Pingoud, A. & Jeltsch, A. *Eur. J. Biochem*. **246**, 1–22 (1997).
24. Gimble, F.S., Duan, X., Hu, D. & Quiocho, F.A. *J. Biol. Chem.* **273**, 30524–30529 (1998).
25. Stephens, K.M., Monnat, R.J., Jr., Heath, P.J. & Stoddard, B.L. *Proteins* **28**, 137–139 (1997).
26. Otwinowski, Z. & Minor, W. *Methods Enzymol*. **276**, 307–326 (1997).
27. Kissinger, C.R. & Gehlhaar, D.K. *EPMR: A program for crystallographic molecular replacement by evolutionary search*. (Agouron Pharmaceuticals, La Jolla, CA; 1997).
28. Brunger, A. *et al. Acta Crystallogr. D* **54**, 905–921 (1998).
29. Brunger, A. *Acta Crystallogr. D* **47**, 24–36 (1993).
30. Laskowski, R.J., Macarthur, M.W., Moss, D.S. & Thornton, J.M. *J. Appl. Crystallogr.* **26**, 383–290 (1993).
31. Carson, M. *Method Enzymol.* **277**, 493–505 (1997).

Human cystatin C, an amyloidogenic protein, dimerizes through three-dimensional domain swapping

Robert Janowski[1], Maciej Kozak[1,2], Elzbieta Jankowska[3], Zbigniew Grzonka[3], Anders Grubb[4], Magnus Abrahamson[4] and Mariusz Jaskolski[1,5]

[1]Department of Crystallography, Faculty of Chemistry, A. Mickiewicz University, Grunwaldzka 6, 60-780 Poznan, Poland. [2]Present address: Department of Macromolecular Physics, Faculty of Physics, A. Mickiewicz University, Umultowska 85, 61-614 Poznan, Poland. [3]Department of Organic Chemistry, University of Gdansk, Sobieskiego 18, 80-952 Gdansk, Poland. [4]Department of Clinical Chemistry, University of Lund, Sweden. [5]Center for Biocrystallographic Research, Institute of Bioorganic Chemistry, Polish Academy of Sciences, Noskowskiego 12/14, 61-704 Poznan, Poland.

The crystal structure of human cystatin C, a protein with amyloidogenic properties and a potent inhibitor of cysteine proteases, reveals how the protein refolds to produce very tight two-fold symmetric dimers while retaining the secondary structure of the monomeric form. The dimerization occurs through three-dimensional domain swapping, a mechanism for forming oligomeric proteins. The reconstituted monomer-like domains are similar to chicken cystatin except for one inhibitory loop that unfolds to form the 'open interface' of the dimer. The structure explains the tendency of human cystatin C to dimerize and suggests a mechanism for its aggregation in the brain arteries of elderly people with amyloid angiopathy. A more severe 'conformational disease' is associated with the L68Q mutant of human cystatin C, which causes massive amyloidosis, cerebral hemorrhage and death in young adults. The structure of the three-dimensional domain-swapped dimers shows how the L68Q mutation destabilizes the monomers and makes the partially unfolded intermediate less unstable. Higher aggregates may arise through the three-dimensional domain-swapping mechanism occurring in an open-ended fashion in which partially unfolded molecules are linked into infinite chains.

Cystatins are single-chain proteins that reversibly inhibit cysteine proteases belonging to the papain (C1) and legumain (C13) families[1,2]. Three types of cystatins are present in higher animals: type 1, without signal peptides (cystatins A and B); the secretory type 2 cystatins (C, D, E, F, S, SN, SA) and the multidomain type 3 cystatins (high and low molecular weight kininogens)[1]. Human cystatin C (HCC) is composed of 120 amino acids[1] and contains, as do other type 2 cystatins, four Cys residues forming two characteristic disulfides (Fig. 1*a*). Wild type HCC is a high-affinity inhibitor of human C1 family enzymes — for example, cathepsins B, H, K, L, and S. In pathological processes, it forms part of the amyloid deposits in brain arteries of young adults, which leads to fatal cerebral hemorrhage[3].

Crystallographic and NMR studies of three cysteine protease inhibitors, chicken cystatin[4–6], cystatin B in complex with papain[7] and cystatin A[8], have revealed similar overall structure, with three regions implicated in interactions with the enzyme (Fig. 1*b*). These regions include the N-terminal segment and two hairpin loops, L1 and L2, that are aligned in a wedge-like fashion. The crystal structure of chicken cystatin[4] (Protein Data Bank (PDB) accession code 1CEW) has defined the general fold of monomeric inhibitors belonging to the cystatin family. Its canonical features include a long α1 helix running across a large, five-stranded antiparallel β-sheet. The connectivity within the β-sheet is: (N)-β1-(α1)-β2-L1-β3-(AS)-β4-L2-β5-(C), where AS is a broad 'appending structure' that is unrelated to the compact core of the molecule and positioned on the opposite ('back side') end of the β-sheet relative to the N-terminus and loops L1 and L2. The development of effective cysteine protease peptide inhibitors for the treatment of *inter alia* tissue-degenerative diseases (like osteoporosis) and bacterial and viral infections[1] would be greatly facilitated by a three-dimensional structure of HCC. Similarly, such a structure is necessary to understand the ability of HCC to inhibit mammalian legumain[9], which is important for antigen processing[10]. The nature of this inhibitory site is unknown, but it does not overlap with the binding site for papain-like proteases and seems to involve residue Asn 39 (ref. 11). Finally, a three-dimensional model of HCC is necessary for the elucidation of the pathophysiological background of the cerebral hemorrhage produced by this protein, particularly its L68Q variant.

Overall architecture of the HCC dimer

Crystallization of full length HCC has been reported by Kozak *et al.*[12]. Our study utilizes the cubic form of HCC crystallized from solutions containing monomeric protein. Chicken cystatin was used as the search model for the preliminary molecular replacement solution. However, it became immediately obvious that the chicken cystatin-like fold in HCC is reconstructed from elements contributed by two HCC monomers (Figs 2*a*,*b*, 3*a*). The crystal structure revealed for the first time how two human cystatin C molecules interact with each other to form a dimer with two identical domains reconstituted from chain fragments contributed by both molecules. The two molecules are related by a crystallographic two-fold rotation, giving a perfectly symmetrical dimer. Since HCC is a monomer in its native functional state (as a cysteine protease inhibitor), and significant amounts of extracellular dimers are present only in pathological conditions[13,14], this structure provides important information about the three-dimensional architecture of the pathological form. A similar structural phenomenon was first observed for diphtheria toxin and was termed three-dimensional domain swapping[15]. Since then, more than a dozen other cases have been described, and three-dimensional domain swapping has been recognized as a mechanism for forming oligomeric proteins from their monomers[16,17].

The HCC dimer is formed through the exchange of three-dimensional 'subdomains' between the two subunits. Each of the two domains thus formed is composed of an α-helix contributed together with one β-strand by one of the molecules and a β-sheet contributed by the other (Figs 1*c*, 2). In the nomenclature of Eisenberg[16], this α–β interface between the two molecules is termed a 'closed interface' because it is identical to that existing in the monomeric protein. The dimers are also stabilized by β-sheet interactions within each domain, formed between strands β3 (in the preserved β-sheet) and β2 (contributed together with the α-helix) (Fig. 1*c*). These interactions also regenerate the monomeric fold and belong to the 'closed interface'. The adhesive forces between the two monomers are not limited to reconstituted monomer-type interactions. Between the two symmetric β2–β3 segments, a new β-sheet is formed by the two linker regions (βL; Ile 56–Gly 59) that correspond in sequence to loop L1 in monomeric chicken cystatin (Fig. 1*b*). The βL–βL sheet forms an 'open interface' — the cohesive new structural feature found only in the HCC dimer. Together, these 'closed interface' and 'open interface' β-interactions result in an unusually long contiguous antiparallel β-sheet formed by two crystallographic copies of strands Tyr 42–Thr 74, which cross from one domain to the other and are involved in as many as 34 main chain hydrogen bonds. There are also hydrogen bond interactions in this region that involve side chains. An NMR study had also demonstrated that HCC dimers are symmetric and suggested a model with a topology similar to that presented here[18], but no atomic coordinates were deposited.

Protein fold

Each domain of the HCC dimer has the general fold of chicken cystatin[4]. The N-terminal subdomain is predominantly α-helical in character, and the C-terminal one is of β-type (Fig. 1). In the α-helical subdomain after a disordered N-terminal segment, the HCC chain forms a short β1 element that leads to the long helix α1. After a connecting loop at residue Asn 39, the chain forms a long β2 strand that leaves the α-subdomain without perturbation of the β-geometry. Through the linker region βL, the β-strand enters the β-subdomain, which consists of three antiparallel β-strands (β3–β5). The βL strand corresponds to the

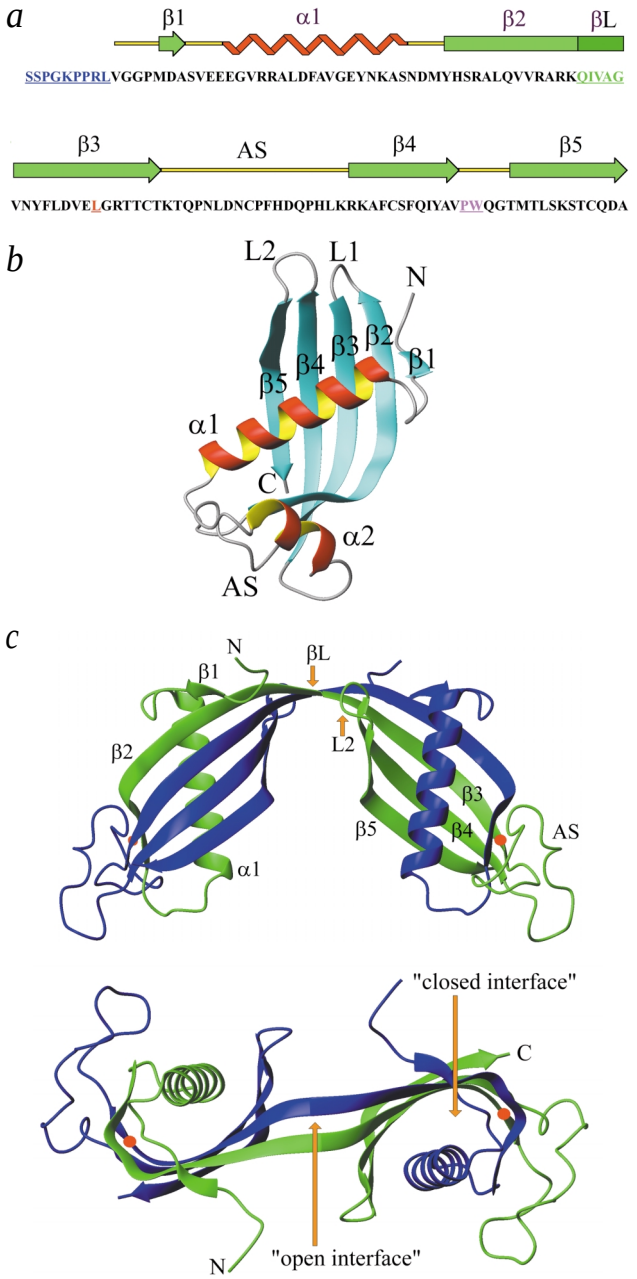

Fig. 1 Primary, secondary, tertiary and quaternary structure of HCC. ***a***, Amino acid sequence of HCC with assignment of secondary structure elements derived from the crystal structure. Blue, N-terminal fragment not visible in electron density; green, linker strand corresponding to loop L1 in monomeric chicken cystatin; magenta, loop L2; red, site of the L68Q mutation. ***b***, The fold of chicken cystatin (PDB entry 1CEW), defining the topology of this class of proteins. ***c***, Domain-swapped dimer of HCC in a view similar to (*b*) (top) and in a perpendicular orientation (bottom) emphasizing the β-sheet in the domain switch region ('open interface') and the site of the L68Q mutation (red dot).

L1 inhibitory loop in the canonical cystatin fold (Fig. 1). The disappearance of loop L1 in the dimeric structure and the consequent disruption of this functional element of the protein agree with the observation that HCC dimers have absolutely no inhibitory effect on C1 type proteases[13].

Two 'back side' loops (contributed by different monomers) form the C-terminal — that is, proximal to the C-terminus of the

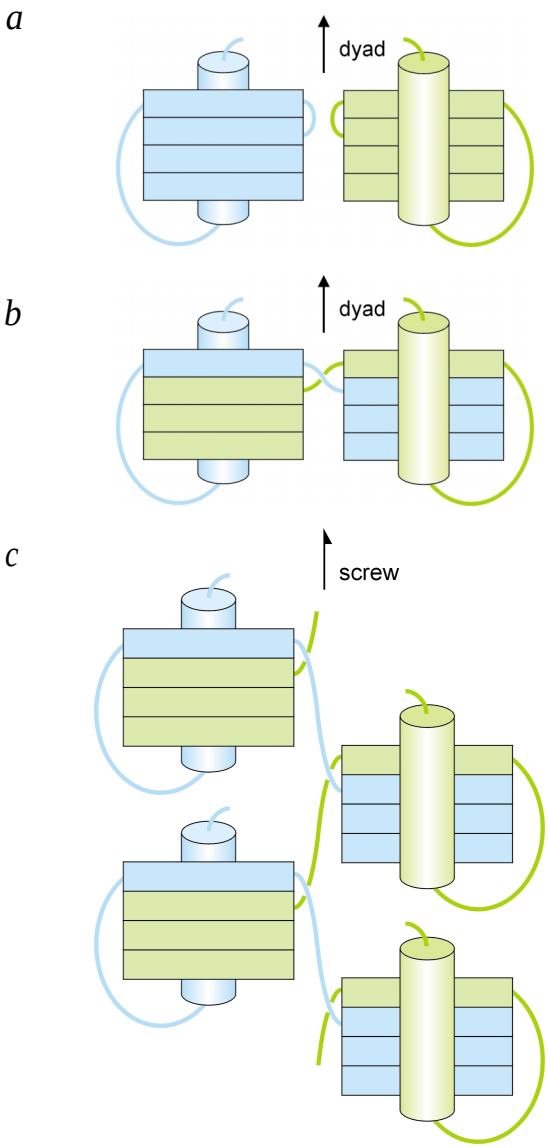

Fig. 2 Schematic illustrations of how HCC oligomers are formed. ***a***, Two monomers form a dimer through ***b***, three-dimensional domain swapping. ***c***, In an open-ended variant, the same mechanism may lead to cross β-fibril structure. In this diagram, the cystatin fold is represented by an α-helix (cylinder) running across the concave face of a β-sheet (stripes). In a screw operation, new components are added by rotation followed by a translation along the screw axis.

polypeptide chain — end of the β-sheet, as opposed to the N-terminal peptide, the L2 loop and presumably the intact L1 loop of the monomeric form, which are located at the N-terminal end of the β-sheet. One of these loops (AS) is broad (residues Lys 75–Lys 92) and only loosely connected with the rest of the protein. It has clear electron density but no secondary structure, in contrast to the same chicken cystatin segment that was poorly visible in electron density and modeled as a helix[6]. The tight 39–41 back side loop is important because it contains a residue (Asn 39) that is crucial for HCC inhibition of mammalian legumain[11]. The back side end of the β-sheet is not perturbed by dimerization, and the affinity of HCC for mammalian legumain should not be affected by dimerization. Indeed, it has been demonstrated that dimeric HCC is as active in inhibiting pig legumain as the monomeric protein[11].

One half (a domain) of the HCC dimer has been compared with the crystal model of chicken cystatin[4]. The α-subdomains of the two structures are very similar; the root mean square (r.m.s.) deviation between the common Cα atoms is 0.5 Å. The similarity is rather poor for the Cα atoms in the β-subdomain (r.m.s. deviation 1.08 Å) but the source of the discrepancy lies in the AS and not in the β-sheet. Overall, the entire half of one HCC dimer is similar to the chicken protein (r.m.s. deviation 0.58 Å for 86 common Cα atoms) confirming: (i) the validity of the cystatin folding canon derived from the structure of chicken cystatin (1CEW); (ii) the fidelity with which the monomer topology is reconstructed after unfolding and dimerization; and (iii) the usefulness of the present dimeric model of HCC for deriving conclusions about the molecular conformation in its native, monomeric state. There are two disulfide bonds in human cystatin C, as in all type 2 cystatins[19,20], and they are preserved in the present dimeric structure. Both bonds are located in the β-subdomain of the molecule and do not interfere with the chain unfolding and dimerization.

Leu 68

Leu 68 is located in the central strand (β3) of the β-sheet, on its concave face and covered by helix α1 (Fig. 1*c*). In the hydrophobic core of the protein, it occupies a pocket formed by the surrounding residues of the β-sheet and the hydrophobic face of the helix (Fig. 3*b*). Its immediate neighbors are Val 66 and Phe 99 of the same monomer, as well as Leu 27, Val 31, Tyr 34 (in the α-helix) and Ala 46 (strand β2) of the complementary monomer. These residues make hydrophobic van der Waals contacts with Leu 68. Replacement of the Leu side chain by the longer Gln side chain, as in the naturally occurring L68Q variant, would not only make these contacts prohibitively close but would also place the mutated hydrophilic chain in a hydrophobic environment. This would most likely destabilize the molecular α–β interface. Model building studies illustrate that a long, chemically incompatible side chain at position 68 would exert a repulsive force on the α-helix, thus expelling it, together with the intervening strand β2, from the compact molecular core and forcing the molecule to unfold into the α- and β-subdomains (Figs 1*c*, 3*b*). This explains the increased dynamic properties of the L68Q mutant compared to wild type HCC observed by NMR spectroscopy[18,21]. Under the assumption that the refolded dimer recreates the topology of monomeric HCC, these destabilizing effects would be similar in both cases. However, the dimeric structure may be more resistant to destruction because of the extra stabilizing contribution from the β-interactions in the linker region, or more generally in the β2–βL–β3 region. A hydrophilic substitution at the α–β interface would also be expected to lower the energy barrier of the unfolded state[16] by reducing the unfavorable solvent contacts of the newly exposed interface. This agrees with the observation that the L68Q variant forms dimers in human body fluids more easily than wild type HCC[14].

Implications for higher oligomeric states

The protein used for growing the crystals[12] in this study was monomeric HCC because gel filtration was the final isolation step. Therefore, the dimerization process must have taken place during crystallization. This is consistent with the view that high local concentrations are necessary for the formation of three-dimensional domain-swapped dimers[22]. On the other hand, wild type HCC can also be prepared in purely dimeric form by mild

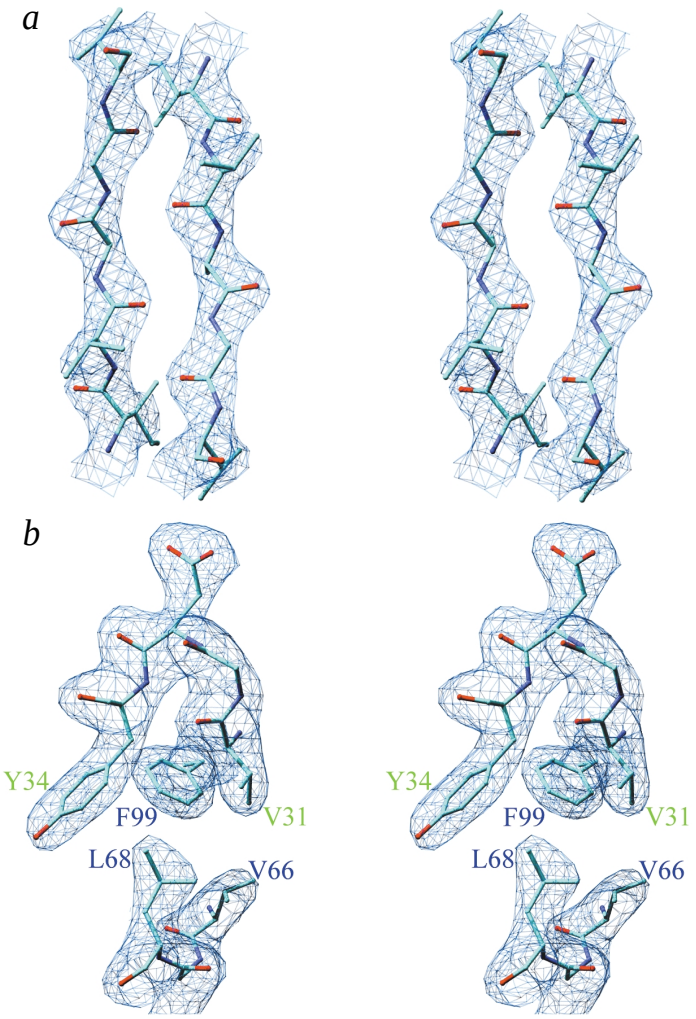

Fig. 3 Electron density maps. ***a***, The linker region across the 4_2-axis forming the 'open interface' (residues Ile 56–Val 60) shown in a $2mF_o - DF_c$ map contoured at the 2.0 σ level. ***b***, A $2mF_o - DF_c$ map (contoured at the 1.5 σ level) for Leu 68 showing its placement in a hydrophobic pocket formed by residues of the β-sheet of one molecule (blue labels) and the α-helix of the other molecule of the dimer (green).

chemical denaturation, at elevated temperature or low pH[23]. This process is more easily achieved with the L68Q variant of the protein because its dimeric form is more stable than the monomeric form even under physiological conditions[13,21]. Dimers of the L68Q mutant are present in body fluids of patients with hereditary cystatin C amyloid angiopathy, which leads to fatal brain hemorrhage in early adult life[14].

If the general fold of monomeric HCC resembles that determined for the chicken analog[4], then why and how does the polypeptide chain unfold and subsequently refold into a higher oligomeric state? The present structure offers important insight. The similarity between the HCC dimer and a pair of chicken cystatin monomers suggests that the unfolding-oligomerization transformation proceeds with maximal retention of the secondary structure. The only drastic conformational change would be restricted to loop L1. A hinge movement of L1 would tear the β2–β3 seam of the β-sheet, resulting in the separation of the α-and β-structures. Reconstruction of the α–β interactions from segments belonging to separate molecules would then give rise to oligomerization.

In the case of dimerization, the two interacting molecules reconstitute the two monomeric topologies in a symmetric fashion, as in the present structure. However, it is very unlikely that such a symmetric dimer would be the first intermediate in the process of higher oligomerization. This is probably a dead-end product in the oligomerization pathway, which would explain the stability of the dimers and the ease with which they can be purified. The energetic advantage of the symmetric dimer may be related to the formation of the strong β-sheet interactions at the 'open interface'. Unhampered chain-like oligomerization could start with the reconstruction of only one α–β domain, leaving the other two α- and β-structures available for interactions with additional monomers (Fig. 2*c*). The assumption that symmetric dimerization, while following the general mechanism of unfolding-refolding, is a suicidal trap on the pathway to higher oligomeric states is corroborated by the difficulty of growing well-diffracting — that is, well-ordered — crystals of HCC[12]. It is possible that monomeric HCC cannot be crystallized because of its conversion into aggregates. Of these, the symmetric dimers are likely to form homogeneous, ordered crystals but the presence of other aggregates would reduce the concentration of the crystallizable dimers and contaminate the solution, preventing sustained growth of well-ordered crystals. Partially unfolded L68Q HCC monomers with largely retained secondary structure have been observed in solution by CD and NMR techniques as distinct molten globule-like intermediates on the unfolding pathway[21].

There is nothing obvious in the HCC sequence (or the 1CEW structure) of the L1 loop to suggest why it is predisposed to destabilization. However, the source of monomer instability may be located elsewhere, possibly at the α–β interface. The observation of the reduced monomer stability and facilitated dimerization of the L68Q mutant suggests that this interpretation may be correct.

In their analysis of the different 'open interfaces' in dimeric RNase A and bull seminal (BS)-RNase, which share the same 'closed interface', Liu *et al.*[22] argue that three-dimensional domain swapping is sufficient for protein oligomerization but that the precise orientation of the subunits is influenced by interactions in the 'open interface'. This lends a possibility to control the overall structure through the use of carefully placed mutations. These remarks are valid and have been illustrated by engineering CD2 mutants for stability and assembly of domain-swapped oligomers[24]. However, the example of HCC and its L68Q mutant suggests that the interplay of kinetic and thermodynamic factors governing the formation of three-dimensional domain swapped oligomers also involves residues in the 'closed interface'. In the case of HCC, the L68Q substitution can be expected to decrease the energy necessary for the transition from the monomeric to dimeric form by: (i) destabilizing the monomer (higher energy) and (ii) lowering the barrier of the transition state (less unfavorable interactions with solvent in the open conformation). Although sealed by strong β-sheet hydrogen bonds, the 'open interface' of our dimer structure presented here is rather small. It is possible that in the process of higher oligomerization, a different 'open interface' could be formed while preserving the 'closed interface'. One might hypothesize that a different conformation of the linker could allow the molecules to aggregate in an open-ended fashion (see Fig. 2*c*). Such a hypothetical model would be compatible

Table 1 Data processing and structure refinement statistics

Space group	I432
Cell parameter (Å)	140.5
Temperature (K)	100
Resolution[1] (Å)	20.0–2.5 (2.59–2.50)
Measured reflections	167,936
Unique reflections	8,429
Completeness[1] (%)	99.2 (93.5)
I / σ[1]	27.8 (2.5)
R_{int}[1,2]	0.070 (0.413)
Refinement statistics	
Resolution range (Å)	20.0–2.5
Number of reflection used	8,429
R-factor[3]	0.216
R_{free}[4]	0.249
Number of atoms	
Protein	871
Water	22
Other[5]	7
R.m.s. deviations from ideality	
Bond lengths (Å)	0.015
Bond angles (°)	1.9
Ramachandran plot statistics (%)	
Most favored regions	90.7
Allowed regions	9.3

[1]Values in parentheses correspond to the last resolution shell.
[2]$R_{int} = \Sigma_h\Sigma_j|I_{hj} - \langle I_h\rangle| / \Sigma_h\Sigma_j I_{hj}$, where I_{hj} is the intensity of observation j of reflection h.
[3]$R = \Sigma_h ||F_o| - |F_c|| / \Sigma_h |F_o|$ for all reflections, where F_o and F_c are observed and calculated structure factors, respectively.
[4]R_{free} was calculated against 10% of all reflections randomly excluded from the refinement.
[5]One glycerol molecule and one chloride ion.

with the experimentally confirmed cross β-structure of amyloid fibrils in which the β-strands are perpendicular and the faces of the β-sheets parallel to the fiber axis[25,26].

Methods

Crystallization and data collection. Single crystals of intact HCC were grown from solutions of the monomeric protein as described[12]. The pH of the crystallization droplets was 4.8 and the precipitating agent, 2-methyl-2,4-pentanediol (MPD), was present only in the reservoir. Low temperature diffraction data extending to 2.5 Å resolution were measured for a cubic polymorph using the BW7B EMBL beamline at the DESY synchrotron. Cryoprotection was achieved by immersing the crystal in the reservoir solution supplemented with 20% (v/v) MPD and 15% (v/v) glycerol. The data were integrated and scaled in the HKL package[27].

Structure determination. The solution of the crystal structure was based on the crystallographic model of chicken cystatin[4] (PDB entry 1CEW). For molecular replacement calculations, the diffraction data were restricted to the 15–4 Å range, and the model was converted to polyalanine. Molecular replacement calculations based on genetic algorithms[28] clearly revealed only one molecule in the asymmetric unit. The refinement started from the monomeric 1CEW model rebuilt to correspond to the HCC sequence. Using 10–3.3 Å data, this model could only be refined to an R-factor of 0.31.

Structure rebuilding and refinement. The molecular replacement located the chicken cystatin model very close to the crystallographic 4_2 axis, which generated exceptionally short contacts between the L1 loops from symmetry related molecules. However, the presence of strong, contiguous $2mF_o - DF_c$ and $mF_o - DF_c$ electron density in the loop L1 region clearly indicated that the connectivity within a two-fold symmetric pair of molecules was different. An omit map excluding residues Ala 53–Tyr 62 confirmed the assumption that the protein chain does not form loop L1 but goes straight in the direction of the second molecule leading to a symmetric (crystallographic) dimer with swapped domains. After rebuilding in O[29], the final model in the chain switch area had very good $2mF_o - DF_c$ density (Fig. 3*a*) and no negative $mF_o - DF_c$ density, even at the –2.0 σ level. Except for the first nine amino acids, which are not seen due to disorder, the protein main chain for residues Val 10–Ala 120 had contiguous $2mF_o - DF_c$ density at the 1.5 σ level. The quality of the electron density maps allowed the modeling of 22 water molecules, one molecule of glycerol and one chloride ion. The rebuilt model was refined in CNS[30] using all available data. The data processing and structure refinement statistics are shown in Table 1.

Coordinates. The coordinates of HCC have been deposited with the PDB (accession code 1G96).

Acknowledgments
The research of M.J. was supported by an International Research Scholar's award from the Howard Hughes Medical Institute. This research was sponsored by grants from the State Committee for Scientific Research, from the Swedish Medical Research Council, and from the A. Osterlund, A. Pahlsson and J. Kock Foundations. We thank V. Lindström, A.-C. Löfström, B. Gerhartz, and M. Alvarez-Fernandez for assistance with protein expression and purification, G. Bujacz for help with data collection, and Z. Otwinowski for advice on data processing.

Correspondence should be addressed to M.J. *email: mariuszj@amu.edu.pl*

Received 29 November, 2000; accepted 13 February, 2001.

1. Grubb, A.O. *Adv. Clin. Chem.* **35**, 63–99 (2000).
2. Turk, V. & Bode, W. *FEBS Lett.* **285**, 213–219 (1991).
3. Olafsson, I. & Grubb, A. *Amyloid Int. J. Exp. Clin. Invest.* **7**, 70–79 (2000).
4. Bode, W. *et al. EMBO J.* **7**, 2593–2599 (1988).
5. Dieckmann, T. *et al. J. Mol. Biol.* **234**, 1048–1059 (1993).
6. Engh, R.A. *et al. J. Mol. Biol.* **234,** 1060–1069 (1993).
7. Stubbs, M.T. *et al. EMBO J.* **9**, 1939–1947 (1990).
8. Martin, J.R. *et al. J. Mol. Biol.* **246**, 331–343 (1995).
9. Chen, J.-M. *et al. J. Biol. Chem.* **272**, 8090–8098 (1997).
10. Manoury, B. *et al. Nature* **369**, 695–699 (1998).
11. Alvarez-Fernandez, M. *et al. J. Biol. Chem.* **274**, 19195–19203 (1999).
12. Kozak, M. *et al. Acta Crystallogr. D* **55**, 1939–1942 (1999).
13. Abrahamson, M. & Grubb, A. *Proc. Natl. Acad. Sci. USA* **91**, 1416–1420 (1994).
14. Bjarnadottir, M. *et al. Amyloid Int. J. Exp. Clin. Invest.* **8**, **in the press** (2001).
15. Bennett, M.J., Choe, S. & Eisenberg, D.S. *Proc. Natl. Acad. Sci. USA* **91**, 3127–3131 (1994).
16. Schlunegger, M.P., Bennett, M.J. & Eisenberg, D. *Adv. Protein Chem.* **50**, 61–122 (1997).
17. Bennett, M.J., Schlunegger, M.P. & Eisenberg, D. *Protein Sci.* **4**, 2455–2468 (1995).
18. Ekiel, I. *et al. J. Mol. Biol.* **271**, 266–277 (1997).
19. Rawlings, N.D. & Barrett, A.J. *J. Mol. Evol.* **30**, 60–71 (1990).
20. Ni, J. *et al. J. Biol. Chem.* **273**, 24797–24804 (1998).
21. Gerhartz, B., Ekiel, I. & Abrahamson, M. *Biochemistry* **37**, 17309–17317 (1998).
22. Liu, Y., Hart, P.J., Schlunegger, M.P. & Eisenberg, D. *Proc. Natl. Acad. Sci. USA* **95**, 3437–3442 (1998).
23. Ekiel, I. & Abrahamson, M. *J. Biol. Chem.* **271**, 1314–1321 (1996).
24. Murray, A.J., Head, J.G., Barker, J.J. & Brady, R.L. *Nature Struct. Biol.* **5**, 778–782 (1998).
25. Bonar, L., Cohen, A.S. & Skinner, M.M. *Proc. Soc. Exp. Biol. Med.* **131**, 1373–1375 (1969).
26. Teplow, D.B. *Amyloid Int. J. Exp. Clin. Invest.* **5**, 121–142 (1998).
27. Otwinowski, Z. & Minor, W. *Methods Enzymol.* **276**, 307–326 (1997).
28. Kissinger, C.R., Gehlhaar, D.K. & Fogel, D.B. *Acta Crystallogr. D* **55**, 484–491 (1999).
29. Jones, T.A., Zou, J.-Y., Cowan, S.W. & Kjeldgaard, M. *Acta Crystallogr. A* **47**, 110-119 (1991).
30. Brunger, A.T. *et al. Acta Crystallogr. D* **54**, 905–921 (1998).